# FLOATING LIDAR ASSESSMENT OF ATMOSPHERIC STABILITY IN THE NORTH SEA

*Araújo da Silva, M. P.* [1], *Student Member, IEEE, Rocadenbosch, F.* [1,2], *Senior Member,* IEEE, *Farré-Guarné, J.* [1], *Salcedo-Bosch, A.* [1], *González-Marco, D.* [3,4], *and Peña, A.* [5]

[1]CommSensLab-UPC, Department of Signal Theory and Communications (TSC),

Universitat Politècnica de Catalunya (UPC), E-08034, Barcelona, Spain;

[2]Institut d'Estudis Espacials de Catalunya (Institute of Space Studies of Catalonia, IEEC),

E-08034, Barcelona, Spain;

[3] Laboratori d'Enginyeria Marítima, Universitat Politècnica de Catalunya, E-08034, Barcelona, Spain;

[4] Centre Internacional d'Investigació dels Recursos Costaners (CIIRC), E-08034, Barcelona, Spain;

[5] DTU Wind Energy, Technical University of Denmark, Frederiksborgvej 399, 4000 Roskilde, Denmark.

Correspondence: marcos.silva@upc.edu (M.P.A.S.); roca@tsc.upc.edu (F.R.)

## ABSTRACT

In this work, the 2D parametric-solver algorithm [1] used to assess atmospheric stability from floating Doppler wind lidar (FDWL) measurements is revisited. The algorithm performance is studied using data

---

This research is part of the projects PGC2018-094132-B-I00 and MDM-2016-0600 ("CommSensLab" Excellence Unit) funded by Ministerio de Ciencia e Investigación (MCIN)/ Agencia Estatal de Investigación (AEI)/ 10.13039/501100011033/ FEDER "Una manera de hacer Europa". The work of M.P Araújo da Silva was supported under Grant PRE2018-086054 funded by MCIN/AEI/10.13039/501100011033 and FSE "El FSE invierte en tu futuro". The work of A. Salcedo-Bosch was supported under grant 2020 FISDU 00455 funded by Generalitat de Catalunya—AGAUR. The European Commission collaborated under projects H2020 ACTRIS-IMP (GA-871115) and H2020 ATMO-ACCESS (GA-101008004).

from IJmuiden campaign. Mast-measured temperature and wind-speed provided the reference parameters used to evaluate the performance of the stability estimation algorithm. From 5,922 10-min samples available, the algorithm classified the atmosphere as stable (52% of the cases), neutral (31%) and unstable (17%), which successfully agreed with the mast-derived reference classification (53%, 30% and 17%, respectively).

***Index Terms***— Floating Doppler wind lidar, Obukhov length, wind energy, atmospheric stability

## 1. INTRODUCTION

In the last decades, the wind energy industry has shown a rising interest in offshore environments due to the strong uniform winds observed over the sea. Meteorological masts installed on the seabed have traditionally been employed for assessing the wind resource in potential wind-farm deployment sites. However, masts require high manufacturing and deployment costs which can easily reach millions of Euro.

Recently, Doppler wind lidars (DWLs) have been accepted as potential substitutes of masts due to their cost-effectiveness and versatility [2]. When sited atop floating buoys, floating DWLs (FDWLs) offer several advantages over masts, such as reduced installation costs (hundreds of thousand Euro), easy redeployment, and shorter installation time. In contrast, off-shore masts are constrained to be deployed in fixed locations and their installation produces higher environmental impact to the seabed. However, overall, FDWLs cannot assess the same number of atmospheric parameters as masts, such as the atmospheric stability, which influences different aspects of the wind power generation, e.g., turbine power performance, wind shear, and wakes [3, 4].

The Obukhov length is widely applied in wind-energy studies to predict the vertical wind-profile shape and to classify the atmospheric stability in different regimes [3, 5]. Obukhov-length estimation is usually carried out by means of sonic-anemometer observations, from which heat fluxes and momentum can directly be retrieved [6]. Alternative methods to assess the Obukhov length have been developed to overcome situations in which the experimental setup is limited [7, 8]. Recently, the companion paper by Araújo da Silva et al. [1] has introduced a 2D parametric algorithm along with data screening criteria as a method to assess the atmospheric stability from solely FDWL-measured wind profiles. Differently from [7], the 2D algorithm retrieves the stability without using temperature observations. Moreover, it can be extended to an unlimited number of measurement heights, which is complementary to [8].

In this work we summarise the 2D algorithm description and evaluate its performance with reference to the mast-derived stability reference. The comparisons are carried out by using a simplified atmospheric stability classification consisting of only three types, namely stable, neutral and unstable.

## 2. MATERIALS AND METHODS

### 2.1. Materials

From April to June 2015 (82 days), the EOLOS$^{TM}$ FDWL pre-commercial buoy was deployed at the IJmuiden test site in the North Sea (52.848 N, 3.436 E). The observational campaign aimed to validate the EOLOS$^{TM}$ FDWL against the reference IJmuiden mast ([1]). The EOLOS$^{TM}$ buoy hosted a ZephIR$^{TM}$ 300 focusable continuous-wave Doppler lidar measuring the wind profile at four heights (25, 38, 56 and 83 m) as well as multiple sensors measuring the buoy's attitude. The IJmuiden mast hosted cup and sonic anemometers, measuring the horizontal wind speed (HWS) at 27, 58.5, and 85 m, along with pressure, temperature and humidity sensors, among others ([5]). Additionally, a TRIAXYS$^{TM}$ buoy was deployed next to the mast measuring ocean-related parameters.

### 2.2. Methods

*Monin-Obukhov similarity theory.-* According to the Monin-Obukhov similarity theory (MOST), the diabatic wind profile at every height $z$ is formulated as

$$U(z) = \frac{u_*}{\kappa}\left[\ln\left(\frac{z}{z_0}\right) - \Psi_m\left(\frac{z}{L}\right)\right], \tag{1}$$

where $u_*$ is the friction velocity [m/s], $\kappa \simeq 0.4$ is the Von Kármán constant, $z_0 = \alpha u_*^2/g$ is the roughness length ($\alpha = 0.012$ is the Charnock's parameter and $g = 9.81$ [m/s$^2$] is the gravitational acceleration), $L$ is the Obukhov Length [m], and $\Psi_m\left(\frac{z}{L}\right)$ is the stability-correction function, which is defined by parts according to the stability type as

$$\Psi_m\left(\frac{z}{L}\right) = \begin{cases} -6\frac{z}{L}, \text{ for } \frac{z}{L} > 0 \text{ (stable)} \\ 0, \text{ for } \frac{z}{L} = 0 \text{ (neutral)} \\ 2\ln(\frac{1+x}{2}) + \ln(\frac{1+x^2}{2}) - 2\arctan(x) + \frac{\pi}{2}, \\ \text{ for } \frac{z}{L} < 0 \text{ (unstable)} \end{cases}, \quad (2)$$

where $x = \left(1 - \frac{19.3z}{L}\right)^{1/4}$. The stability types are defined in Table 1, which is a simplified form of the stability classification defined by Gryning et al. [9]. The very-stable, near-neutral and very-unstable classes defined in [9] were aggregated into stable, neutral and unstable, respectively. The excluded interval $-50 < L < 10$ skips the singularity of Eq. (1) for $L \to 0$.

**Table 1**. Stability classes based on the Obukhov length, $L$.

| **Atmospheric Stability** | **Obukhov length range (m)** |
|---|---|
| Stable | $10 < L < 500$ |
| Neutral | $\|L\| > 500$ |
| Unstable | $-500 < L < -50$ |

*Parametric wind-model estimation.-* The 2D parametric algorithm by Araújo da Silva et al. [1] optimises the variables $L$ and $u_*$ of the MOST diabatic wind-profile model in order to fit the model to the FDWL-measured wind profile. The optimisation problem is formulated as

$$(L, u_*) = \underset{L,u_*}{arg\ min}||\vec{U}_{FDWL} - \vec{U}(L, u_*)||^2, \quad (3)$$

where the function $\vec{U}(L, u_*)$ is the parametric wind profile model formulated by (Eq. 1) and piece-wise by (Eq. 2). A constrained non-linear least squares (NLSQ) method is used to solve the model parameters, $L$, and $u_*$, by minimising the error norm between the model vector, $\vec{U}(z)$, and the FDWL-measurement vector, $\vec{U}_{FDWL}$. Two search branches, one with a positive-$L$ starting point ($L^+ = 500$) and another with a negative-$L$ starting point ($L^- = -500$), are considered for enhanced sensitivity of the algorithm and avoiding the asymptotic discontinuity of $\Psi_m\left(\frac{z}{L}\right)$ at $L = 0$. The vector with the smallest error norm is chosen as the solution.

*Reference stability.-* The Obukhov length is usually computed from temperature and three-component wind-velocity data [6]. Although all these variables can directly be measured by sonic anemometers, only wind-velocity observations were available during the IJmuiden campaign (i.e., sonic-anemometer temperature was not stored). For this reason, the alternative method [10] to retrieve Obukhov length via the bulk Richardson number ($Ri$) is followed next. This approach has also been used in recent studies [5]. In practice, the $Ri$ is retrieved from mast-derived temperature, pressure, and humidity measurements, and wave-buoy-measured water temperature [1].

*Data screening.-* Outliers in the FDWL measurements are identified by plotting the HWS differences between the FDWL and mast observations as a function of different FDWL internal parameters such as the backscatter, bearing, points in fit, and spatial variation (SV). The greatest HWS differences were attributable to bearing and SV, the SV being a turbulence indicator within the lidar scan circle. The following outlier rejection criteria were applied: (i) HWS $< 2$ [m/s] or HWS $> 100$ [m/s] (ZephIR$^{\text{TM}}$ 300 specs), (ii) bearing = $0$ deg (FDWL compass issue), and (iii) spatial variation above the 95th percentile (equivalently, SV$\geq 0.05$).

## 3. DISCUSSION RESULTS

During the 82-day IJmuiden campaign, a 10,833 10-min samples dataset was produced. The performance of the 2D algorithm for the estimated Obukhov length, $\hat{L}$, was tested against the bulk-Richardson reference, $L_{Ri}$, for the whole campaign. After applying the outlier rejection criteria presented in Sect. 2 above and rejecting Obukhov-length values out of the ranges of Table 1 ($-50 < L < 10$) for both $\hat{L}$ and $L_{Ri}$, we obtained a 5,922-sample "clean" dataset. Nearly identical stability classification results were obtained when comparing $\hat{L}$ to $L_{Ri}$ for the whole campaign: 52% ($\hat{L}$) vs. 53% ($L_{Ri}$) of the cases were classified as stable, and 31% ($\hat{L}$) vs. 30% ($L_{Ri}$) as neutral; the unstable cases remained essentially the same, 17%.

Next, Figure 1 plots the one-to-one correspondence between the estimated and reference classes (as derived from $\hat{L}$ and $L_{Ri}$, respectively) by means of a confusion matrix. The matrix rows and columns represent the instances in an actual reference stability class and the instances in the corresponding estimated class, respectively. An ideal predictive estimation would have all instances along the principal diagonal of the confusion matrix.

Figure 1a shows the results considering the seven stability classes defined in Gryning et al. [9], and Figure 1b the results considering the three classes defined in Table 1. Overall, much higher hit hates were achieved when considering only these three classes, as shown by the summary matrices. For instance, the

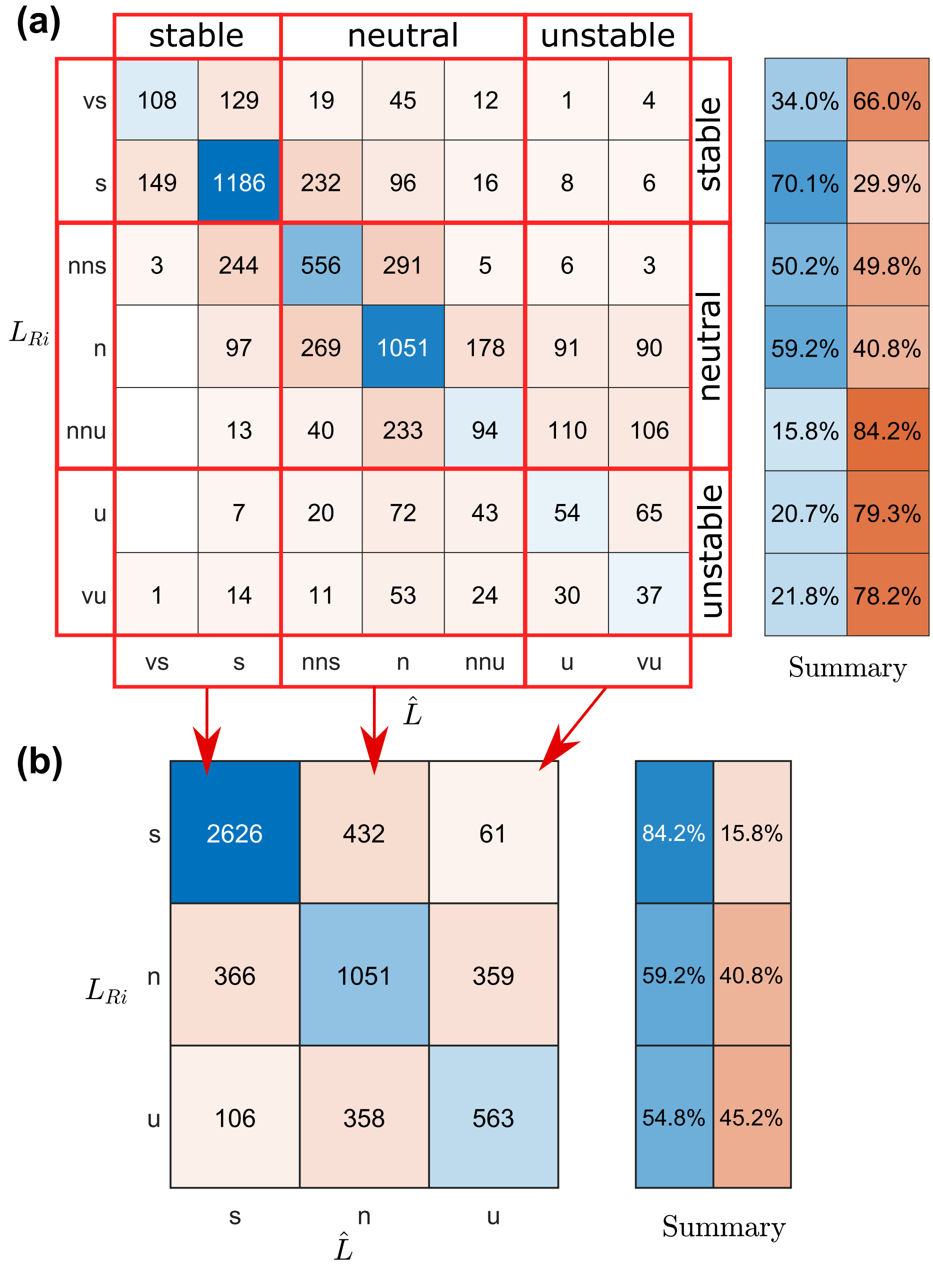


**Fig. 1**. Confusion matrix between $\hat{L}$ and $L_{Ri}$. (a) According to the stability classes in Gryning et al. [9] (b) Class regrouping of panel (a) matrix (Table 1). In both panels the summary matrix on the right totals the hit rates (bluish) and miss rate (reddish) for each class. (vs), very stable; (s), stable; (nns), near-neutral stable; (n), neutral; (nnu), near-neutral unstable; (u), unstable; (vu), very unstable. Red rectangles in (a) delimit panel (b) matrix cells after class regrouping.

"near-neutral unstable" (nnu) and "unstable" (u) classes in Figure 1a yielded hit rates lower than 22%, whereas when these two classes were aggregated into a single class named "unstable" (Figure 1b), the hit hate increased to $\approx 55\%$. The poor performance for the (vs), (nnu), (u) and (vu) classes in Figure 1a is attributed to wind profiles often indistinctly misclassified into adjacent classes [1]. In addition, Figure 1b shows that in spite of the good hit rates achieved for the whole campaign there is substantial cross-classification between right- and left-adjacent classes to the main diagonal.

Furthermore, Figure 2 compares the stability classification results clustered by hour of the day. Overall, Figure 2a and b show similar order of magnitude for all classes over the course of the day. However, the neutral and unstable classes estimated by the 2D algorithm around the 5-to-15-UTC time window (local time is UTC+1) were slightly overestimated in relation to the Richardson reference.

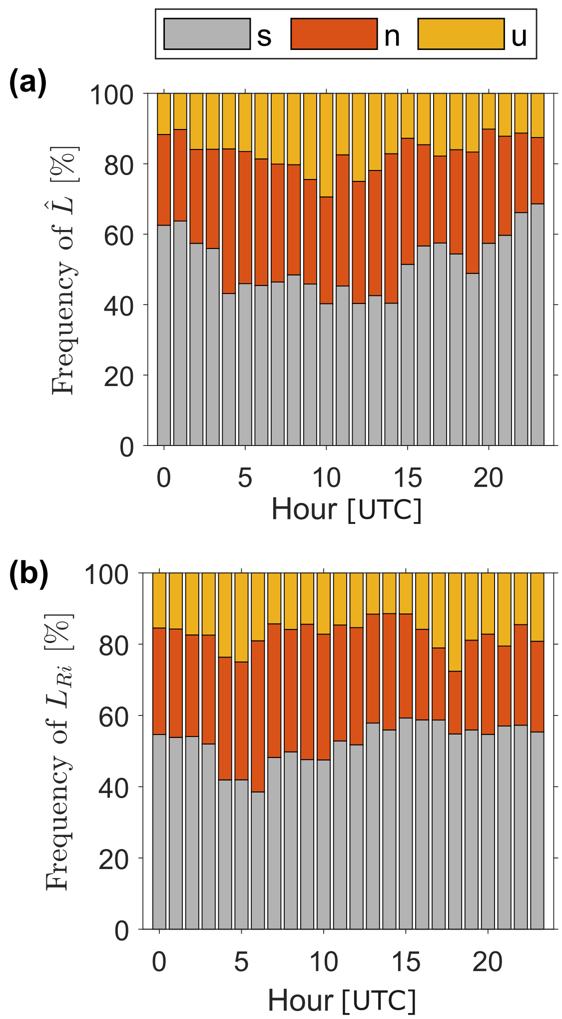


**Fig. 2**. Frequency of occurrence of each stability class clustered by hour of the day. (a) Estimated Obukhov length, $\hat{L}$. (b) Richardson reference, $L_{Ri}$. (s, n and u) stand for stable, neutral and unstable, respectively.

Finally, successful results were also obtained when comparing the frequencies of occurrence of the estimated and reference stability classes as a function of HWS in Figure 3. The 2D algorithm provided highly similar stability clusters versus HWS. However, the algorithm overestimated the neutral class for the 26-m/s HWS cluster (Figure 3a) to the detriment of the stable class when compared to the Richardson reference (Figure 3b). In addition, both the 2D and the Richardson reference showed that the neutral class was prominent for the highest HWSs, whereas stable and unstable classes were associated to the lowest HWSs.

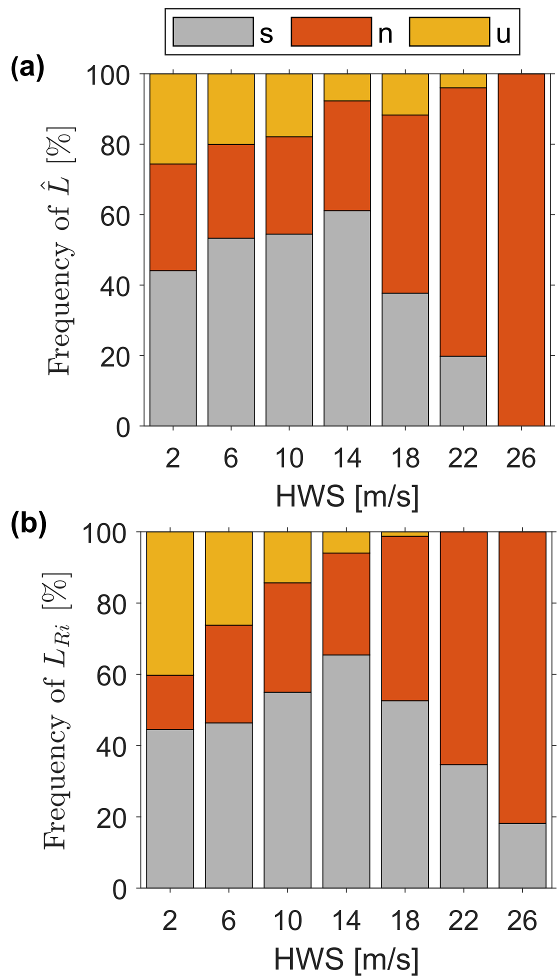


**Fig. 3**. Frequency of occurrence of each stability class clustered by horizontal wind speed (HWS). Labels as in Fig. 2

## 4. CONCLUSION

The 2D algorithm [1] for atmospheric stability estimation from FDWL-measured wind profiles was revisited in the context of two stability categorisations, the Gryning's (seven subclasses) and the stable-neutral-unstable (three classes) from Table 1. The algorithm consists of fitting the MOST wind profile model to the measured FDWL wind profile using a constrained non-linear least squares optimisation and FDWL data screened along the filtering criteria outlined in Sect. 2. When the Gryning's subclasses were aggregated into the s-n-u classes the results substantially improved, thus achieving overall hit rate was as high as 72% (84%, 59%, and 55%, respectively). When comparing the 2D-estimated Obukhov length with the mast-derived reference for the stability evolution during the time of day (Figure 2) and horizontal-wind-speed dependence on the stability class (Figure 3) fairly similar results were also obtained. All in all, this work showed the potential of the FDWL as a standalone instrument to assess the offshore atmospheric stability.

## 5. REFERENCES

[1] M. P. Araújo da Silva, F. Rocadenbosch, J. Farré-Guarné, A. Salcedo-Bosch, D. González-Marco, and A. Peña, "Assessing obukhov length and friction velocity from floating lidar observations: A data screening and sensitivity computation approach," *Remote Sensing*, vol. 14, no. 6, 2022.

[2] Carbon Trust, "Carbon trust offshore wind accelerator roadmap for the commercial acceptance of floating lidar technology," Carbon Trust, Tech. Rep., Oct. 2018, version 2.0.

[3] B. Subramanian, N. Chokani, and R. S. Abhari, "Impact of atmospheric stability on wind turbine wake evolution," *Journal of Wind Engineering and Industrial Aerodynamics*, vol. 176, pp. 174–182, 2018.

[4] D.-Y. Kim, Y.-H. Kim, and B.-S. Kim, "Changes in wind turbine power characteristics and annual energy production due to atmospheric stability, turbulence intensity, and wind shear," *Energy*, vol. 214, p. 119051, 2021.

[5] M. C. Holtslag, W. A. A. M. Bierbooms, and G. J. W. Van Bussel, "Validation of surface layer similarity theory to describe far offshore marine conditions in the dutch north sea in scope of wind

energy research," *Journal of Wind Engineering and Industrial Aerodynamics*, vol. 136, pp. 180–191, 2015.

[6] R. B. Stull, *An introduction to boundary layer meteorology*. The Netherlands: Kluwer Academic Publishers, 1988.

[7] A. C. M. Beljaars, A. Holtslag, and R. Van Westrhenen, *Description of a software library for the calculation of surface fluxes*. KNMI De Bilt, Netherlands, 1989.

[8] S. Basu, "A simple recipe for estimating atmospheric stability solely based on surface-layer wind speed profile," *Wind Energy*, vol. 21, no. 10, pp. 937–941, 2018.

[9] S.-E. Gryning, E. Batchvarova, B. Brümmer, H. Jørgensen, and S. Larsen, "On the extension of the wind profile over homogeneous terrain beyond the surface boundary layer," *Boundary-layer meteorology*, vol. 124, no. 2, pp. 251–268, 2007.

[10] A. Grachev and C. Fairall, "Dependence of the monin–obukhov stability parameter on the bulk richardson number over the ocean," *Journal of Applied Meteorology*, vol. 36, no. 4, pp. 406–414, 1997.